



Design, synthesis and anti-Parkinson evaluation of Ethyl 2-((5-(furan-2-ylmethylene)-4 oxothiazolidin-2-ylidene) amino)-thiazole-4-carboxylate and N'-(4-(benzyloxy)-3-methoxybenzylidene)-2-acetamidothiazole-4-carbohydrazide against neuroleptic induced catalepsy

Rajnish Kumar Malik^a, Tanveer Naved^{a*}, Vikramdeep Monga^b, Amit Kumar Sharma^a

^aAmity Institute of Pharmacy, Amity University, Noida Campus, Uttar Pradesh, India-201313

^bDepartment of Pharmaceutical Sciences and Natural Products, Central University of Punjab, Ghudda, Bathinda, Punjab, India-151401

*Corresponding Author E-mail address: tnaved@amity.edu

Manuscript Received: 15 Jul 2022

Revised: 25 Oct 2022

Accepted: 03 Dec 2022

Abstract

The anti-Parkinsonian and neuroprotective potential of two new derivatives of ethyl 2-aminothiazole-4-carboxylate (SH-4 & SH-9) was investigated in the current work. Based on their spectrum data, the structures of the synthesized compounds were verified. Both substances were discovered to be effective against the catalepsy and oxidative stress brought on by MPTP in mice. Each synthesized compound's potency was predicted computationally, and its *in-vivo* anti-parkinsonian action was then assessed. Both substances have an active binding interaction with α -synuclein, according to the findings of molecular docking. Synthesized substances, namely SH-4 & SH-9, created the most stable complex with α -synuclein by occupying the enzyme's active site and generating hydrogen bonds. An *in-vivo* experiment showed that mice exposed to MPTP took noticeably longer to traverse the beam than the controls. However, supplementation with SH-4 and SH-9 reduced the time it took the animals to traverse the beam and concurrently increased the average velocity. These substances could therefore be considered as potential lead compounds for the development of new and potentially improved MAO-B inhibitors.

Keywords: Parkinson's disease, MPTP, α -synuclein, Ethyl 2-aminothiazole-4-carboxylate derivatives, Ethyl 2-((5-(furan-2-ylmethylene)-4-oxothiazolidin-2-ylidene) amino)-thiazole-4-carboxylate (SH4), N'-(4-(benzyloxy)-3-methoxybenzylidene)-2-acetamidothiazole-4-carbohydrazide (SH-9)

1. Introduction:

The most prevalent neurodegenerative ailment, Parkinson's disease (PD), is characterized by distinctive motor symptoms such as rigidity, tremor, postural instability and bradykinesia. The first who wrote about this disease was James Parkinson in 1817 [1]. Patients with PD may also experience non-motor symptoms include sleep difficulty, psychotic symptoms, sensory abnormalities, mood changes, and cognitive impairment. After the substantia nigra's pars compacta loses its dopaminergic neurons, Parkinson's disease (PD) manifests and is accompanied by intracellular aggregates of misfolded alpha-synuclein [2]. In PD, the substantia nigra's dopaminergic neurons get disappear. The pathologic characteristic of PD is the Lewy body, a neuronal inclusion mostly composed of protein aggregations of the synuclein type. Although several pathways, including as neuroinflammation, oxidative stress, mitochondrial dysfunction, and abnormal protein homeostasis have been suggested as potential causes of PD, its exact cause is still unknown [3,4]. Parkinson's disease motor symptoms are linked to pathology in these regions. Hallucinations and cognitive deterioration become more noticeable as Parkinson's disease progresses and affects the cerebral cortices [2,5].

Monoamine oxidase (MAO) is a flavin adenine dinucleotide-containing enzyme that is located in the outer mitochondrial membrane. Monoamines, which include neurotransmitters including dopamine (DA), epinephrine, and nor-epinephrine, are oxidatively deaminated by MAO. There are two isoforms of MAO: MAO-A and MAO-B. Despite having a 73% sequence similarity, the substrate and inhibitor specificities of these isoforms vary [6]. Serotonin and DA are the usual physiological substrates for MAO-A and MAO-B, respectively. While MAO-B inhibitors are successful in treating Parkinson's disease and Alzheimer's disease, selective MAO-A inhibitors are helpful in the treatment of depression [7]. The cornerstone of medication development for neurodegenerative and neuropsychiatric disorder is the selective and reversible MAO inhibitor (MAOI) [8]. Although effective, the pharmaceutical MAO inhibitors have a number of adverse effects. First and foremost, a hypertensive crisis called the "cheese effect" that happens when tyramine-rich meals are consumed [9]. Rasagiline medication is not linked to the "cheese effect," however it is not recommended for Parkinson's disease patients who have hepatic dysfunction and cannot be coadministered with opioids and antidepressants [8]. Based on the pharmacological significance of MAO-B inhibitors in PD, discovery of new compounds may have enormous therapeutic potential due to their reduced side effects. It has

already been noted that 2-amino-4-substituted thiazoles have anthelmintic, anti-leukotrienes, anticonvulsant, antimalarial and fungicidal effects [10].

Therefore, the purpose of this research was to synthesis a number of new chemicals entities and evaluate their potential impact on several biological receptors involved in PD. The substances that had the greatest affinity for each receptor were then examined in various behavioural paradigms associated with this disease.

2. Material and Method:

2.1 Material

Analytical-grade substances were employed for the study. Levodopa, Ethanol, Chlorpromazine, DTNB reagent, Griess reagent, Bovine serum albumin, Nitric oxide, Serotonin were procured from Sigma Aldrich. Tri chloro acetic acid, Thio barbituric acid, potassium phosphate, Citric acid, Sodium chloride were supplied by SRL Chemicals, Navi Mumbai, Maharashtra. Deprenyl HCl was procured from Thermo Fisher Scientific, Maharashtra. Ethyl acetate, Toluene, Sodium azide, Phenylethylamine, Diphenyloxazole, from P C Chem, Mumbai. Standard pellet diet was supplied by VRK, Nutritional Solutions, Pune, Maharashtra and 1,1,3,3- Tetra Methoxy Propane was procured from Novachem Industries, Mumbai, Maharashtra.

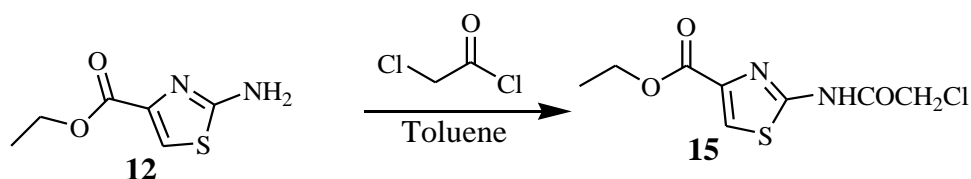
2.2 Method:

2.2.1 General methods for the synthesis of Novel derivatives of ethyl 2-aminothiazole-4-carboxylate

2.2.1.1 Scheme 1-Synthesis of novel Thiazole/Thiazolidinone derivatives

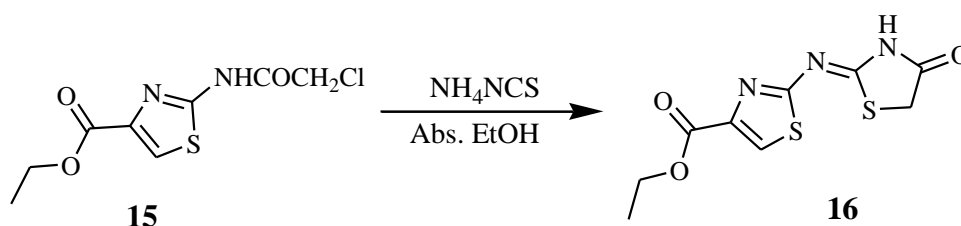
Step 1: Chloroacetylation of ethyl 2-aminothiazole-4-carboxylate

At room temperature, the precursor solution of ethyl 2-aminothiazole-4-carboxylate (12, 0.01mol) in dry toluene (50 mL) was agitated while chloroacetyl chloride (0.015mol) was added dropwise. For 4 to 6 hours, the reaction mixture was heated under reflux. In order to get Ethyl 2-[2-chloroacetamido]-thiazole-4-carboxylate (15) in good yield and purity, the solvent was then evaporated *in vacuo* and the resulting residue was triturated with water, filtered, dried, and then recrystallized from ethanol.



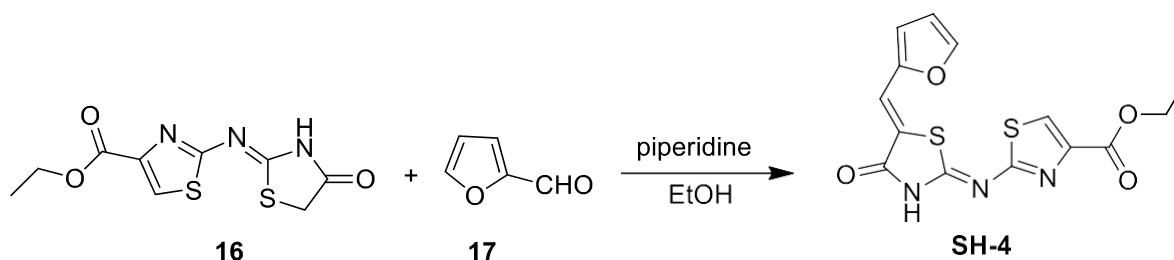
Step 2: Cyclization of Ethyl 2-[2-chloroacetamido]-thiazole-4-carboxylate (15)

Ethyl 2-[2-chloroacetamido]-thiazole-4-carboxylate (**15**, 0.005mol) was refluxed with ammonium thiocyanate (0.010mol) in the presence of absolute ethanol for 3-4 hours. The progress of reaction was monitored by precoated TLC plate. Keep the reaction mixture overnight, after completion. Solvent was then evaporated *in vacuo* and the residue obtained was triturated with water, filtered, dried and recrystallized from absolute ethanol to get the **Ethyl 2-(4-oxothiazolidin-2-ylideneamino)-thiazole-4-carboxylate (16)** in good yield and purity.



Step 3: Condensation of Ethyl 2-(4-oxothiazolidin-2-ylideneamino)-thiazole-4-carboxylate (16) with Furan

A mixture of furan-2-carboxaldehyde (20 mmol) and ethyl 2-[(Z)-(4-oxo-1,3-thiazolidin-2-ylidene) amino]-1,3-thiazole-4-carboxylate (20 mmol) was suspended in absolute ethanol and to this catalytic quantity of piperidine (2 mmol) was added. The mixture was refluxed with stirring at 80 °C for 4 hrs. Percolated TLC plates were used to monitor reaction development. After the reaction was finished, mixture was poured into ice cold water and acidified with glacial acetic acid to pH 3-4 to produce crude solid. The crude product was filtered, washed thoroughly with water and recrystallized from methanol to yield the pure product i.e., **Ethyl 2-((5-(furan-2-ylmethylene)-4-oxothiazolidin-2-ylidene) amino)-thiazole-4-carboxylate (SH-4)**.



2.2.1.1.1 Ethyl 2-[2-chloroacetamido]-thiazole-4-carboxylate (**15**) IR (KBr) ν_{max} (cm^{-1}): 3276 (N-H stretching), 3172 (Aromatic C-H stretching), 2982 (Aliphatic C-H stretching), 1719 (C=O), 1658 (C=O), 1610 (C=N), 1564 (C=C). $^1\text{H-NMR}$ (300 MHz, CDCl_3-d_6): δ (ppm) 10.89 (brs, 1H, NH), 7.87 (s, 1H, Ar-H of thiazole), 4.40 (q, 2H, $J=7.2$ Hz, CH_2), 4.31 (s, 2H, CH_2Cl),

2.17 (s, 3H, CH₃), 1.39 (t, 3H, J = 7.2, CH₃).

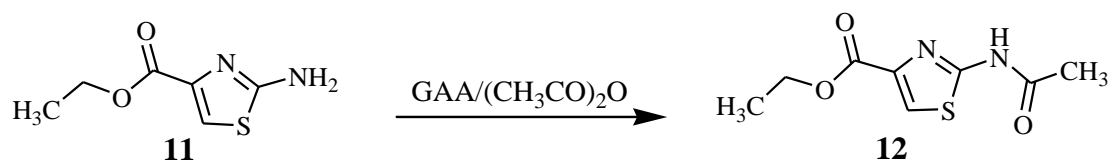
2.2.1.1.2 Ethyl 2-(4-oxothiazolidin-2-ylideneamino)-thiazole-4-carboxylate (16) IR (KBr) ν_{\max} (cm⁻¹): 3284 (N-H stretching), 3184 (Aromatic C-H stretching), 2921 (Aliphatic C-H stretching), 1722 (C=O), 1650 (C=O), 1577 (C=N), 1540 (C=N), 1510 (C=C stretching). ¹H-NMR (300 MHz, CDCl₃): δ (ppm) 11.95 (s, 1H, NH), 7.89 (s, 1H, Ar-H of thiazole), 4.42-4.35 (m, 2H, CH₂CH₃), 3.91 (s, 2H, CH₂ of thiazolidine), 1.42-1.37 (t, 3H, CH₃).

2.2.1.1.3 Ethyl 2-((5-(furan-2-ylmethylene)-4-oxothiazolidin-2-ylidene) amino)-thiazole-4-carboxylate (SH-4) IR (KBr) ν_{\max} cm⁻¹: 3411 (N-H), 2970 (aromatic C-H stretching), 1715 (C=O), 1584 (C=N), 1462 (C=C), 1243 (C-N). ¹H-NMR (300MHz, DMSO-d₆): δ (ppm) 12.64 (s, 1H, N-H); 8.25 (s, 1H, =CH); 8.04 (s, 1H, C₅-H of thiazole); 7.57 (s, 1H, C₅-H of furan); 7.10 (s, 1H, C₃-H of furan); 6.77 (s, 1H, C₄-H of furan); 4.36-4.29 (q, 2H, J = 6.6 Hz, CH₂); 1.38-1.33 (t, 3H, J = 6.6 Hz, CH₃).

2.2.1.2 Scheme 2-Synthesis of Novel Hydrazone Derivatives

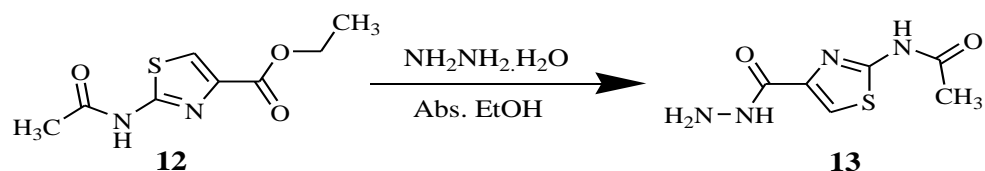
Step 1: Acetylation of Ethyl 2-aminothiazole-4-carboxylate

In the presence of acetic acid anhydride (6 mL), ethyl 2-aminothiazole-4-carboxylate (2 g) was refluxed for about 30 minutes with glacial acetic acid (2 mL). The resulting product was filtered, thoroughly washed in water to remove any remaining glacial acetic acid, and then recrystallized from ethanol to produce the Ethyl-2-acetamido thiazole-4-carboxylate in an excellent yield (83%).



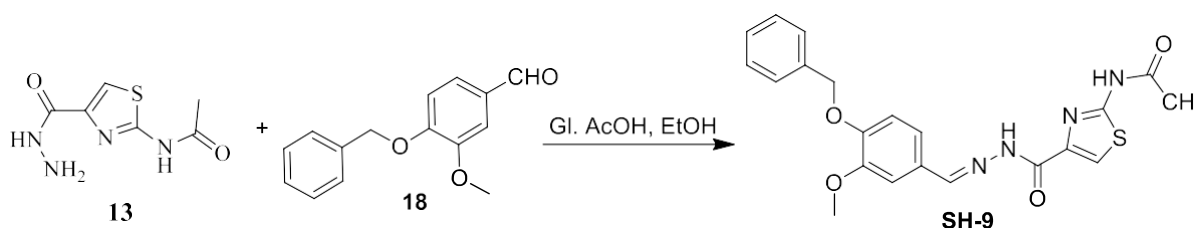
Step 2: Hydrazinolysis of 2-acetamido thiazole-4-carboxylate

The 2-acetamido thiazole-4-carboxylate (0.019mol) was refluxed with hydrazine hydrate (0.056mol) in presence of absolute ethanol for 10 hrs. The white solid so obtained was washed with aq. ethanol to remove excess of hydrazine hydrate and recrystallized from ethanol to yield pure compound.



Step 3: Condensation of Hydrazide with aldehyde to synthesise SH9

Equimolar quantity of 2-acetamido thiazole-4-carbohydrazide (**13**) was refluxed with substituted benzaldehyde **18** in the presence of absolute ethanol and few drops of glacial acetic acid for 14 hrs. The resulting mixture was poured in ice water and solid thus obtained was collected by filtration and washed with water. The crude product was purified by recrystallization from ethanol to afford title compound i.e., N'-(4-(benzyloxy)-3-methoxybenzylidene)-2-acetamidothiazole-4-carbohydrazide (**SH-9**) in satisfactory yield and purity.



2.2.1.2.1 Ethyl-2-acetamido thiazole-4-carboxylate (**12**) IR (KBr) $\nu_{\max}(\text{cm}^{-1})$: 3174 (N-H, stretching), 3072 (Aromatic, C-H stretching), 2982 (Aliphatic, C-H stretching), 1719 (C=O), 1658 (C=O), 1610 (C=N), 1564 (C=C). $^1\text{H-NMR}$ (400 MHz, CDCl_3): δ (ppm) 12.43 (bs, 1H, CONH, D_2O exchangeable), 7.98 (s, 1H, $\text{C}_5\text{-H}$), 4.28-4.21 (q, 2H, CH_2), 2.12 (s, 3H, CH_3), 1.29-1.24 (t, 3H, CH_3).

2.2.1.2.2 2-acetamido thiazole-4-carbohydrazide (**13**) IR (KBr) $\nu_{\max}(\text{cm}^{-1})$: 3411 (N-H stretching), 3284 (N-H, stretching), 3133 (N-H stretching), 3084 (Aromatic C-H stretching), 2921 (Aliphatic C-H stretching), 1662 (NHCOCH_3), 1628 (CONHNH_2), 1613 (C=N), 1568 (C=C stretching). $^1\text{H-NMR}$ (300 MHz, DMSO-d_6): δ (ppm) 12.17 (bs, 1H, NHCOCH_3 , D_2O exchangeable), 9.05 (bs, 1H, NH_2NH , D_2O exchangeable), 7.71 (s, 1H, Ar-H of thiazole), 4.69 (s, 2H, NH_2 , D_2O exchangeable), 2.17 (s, 3H, CH_3). $^{13}\text{C-NMR}$ (300 MHz, DMSO-d_6): δ (ppm) 169.12 ($\text{C}_2\text{-CO}$), 160.65 (C_2), 157.88 ($\text{C}_4\text{-CO}$), 143.50 (C_4), 116.70 (C_5), 22.56 (CH_3).

2.2.1.2.3 N'-(4-(benzyloxy)-3-methoxybenzylidene)-2-acetamidothiazole-4 carbohydrazide (**SH-9**) IR (KBr) $\nu_{\max} \text{cm}^{-1}$: 3216 (N-H), 2972 (aromatic C-H stretching), 1667 (2C=O), 1552 (C=C), 1369 (C-O), 1267 (C-N). $^1\text{H-NMR}$ (300MHz, DMSO-d_6): δ (ppm) 12.31 (s, 1H, N-H); 11.28 (s, 1H, N-H); 8.33(s, 1H, =CH-Ar); 7.92 (s, 1H, $\text{C}_5\text{-H}$ of thiazole); 7.43-7.34 (m, 6H, Ar-H); 7.18-7.10 (m, 2H, Ar-H); 5.13 (s, 2H, $-\text{OCH}_2$); 3.83 (s, 3H, OCH_3); 2.18 (s, 3H, CH_3).

2.2.2 Molecular Docking Study

The three-dimensional X-ray structure of α -synuclein was obtained from RCSB Protein Data Bank. Water molecules and other complexed compounds were taken out of the structure to make it more refined. Using AutoDock Tools-1.5.6, hydrogen atoms were added and electronic charges were given to the protein atoms using the Kollman United Atoms Force Field. Using AUTOTORS, the gasteiger partial atomic charges were added, and all of the ligand's flexible torsion angles were determined. For AutoDock computations, the structures were saved in a

PDBQT format. Both the Lamarckian Genetic Algorithm and the Genetic Algorithm were used to do the docking calculations.

2.2.2.1 Docking Studies and Drug likeness

Docking calculations were performed to predict the binding affinity between the compounds and protein i.e., α -synuclein using AutoDock 4.2. AutoDock requires precalculated grid maps, one for each atom type present in the ligand being docked. These maps were calculated by using the auxiliary program AutoGrid. The compounds treated as flexible molecules were allowed to move in the six spatial degrees of freedom for orientation and torsional degrees of freedom within the grid box. Semi empirical free energy force field are used by AutoDock to evaluate conformations during docking simulations. The energy functions define what contributes to the energy of the molecule, like bond stretching, bending etc., so that energy of the molecule can be calculated for any particular conformation. The force field evaluates binding in two steps. In the first step, the intramolecular energetics is estimated for the transition from unbound states to the conformation of the ligand and protein in the bound state. The second step then evaluates the intermolecular energetics of combining the ligand and protein in their bound conformation.

$$\Delta G = \Delta G_{vdw} + \Delta G_{hbond} + \Delta G_{elec} + \Delta G_{tor} + \Delta G_{desolv}$$

The first three terms are for van der Waal's, hydrogen bonding, electrostatics respectively. The term ΔG_{tor} is for rotation and translation and ΔG_{desolv} is for desolvation upon binding and the hydrophobic effect. Drug-Likeness and molecular property prediction for the compound was done by molsoft [11].

2.2.3 Pharmacological Evaluation- *In-vivo* Anti- Parkinson's Study

The synthesized compounds i.e., SH4 & SH9 were further evaluated for antiparkinsonian activity in animal models. The swiss albino mice (weight-15-20 g) were housed in a well-ventilated room with a 12-hour light/dark cycle in standard poly propylene cages [43 × 27 × 15 (l × b × h) cms] under controlled temperature (26 ± 1°C) and humidity (30%–40%). They were fed with a standard pellet diet obtained from Gold Moher, Lipton India Ltd, Hyderabad and water ad libitum throughout the experimental period. All animal experiments were conducted in compliance with the CPCSEA (Committee for the Purpose of Control and Supervision of Experiments on Animals) guidelines and study was approved by the IAEC (Institutional animal ethical committee). Levodopa (Sigma-Aldrich) was injected i.p. at a dose of 100mg/kg. MPTP was administered to mice as four intraperitoneal (i.p.) injections (20 mg

MPTP/kg body weight) in saline at 2 h intervals in a single day [12-13]. Each group contained 6 animals. Table 1 presented the treatment paradigm. The total dose of MPTP per animal was 80 mg/kg. 7 days before acute MPTP injection, test compound-treated mice received compounds at a concentration of 100 mg/kg body weight by oral gavage.

Table 1: Animal Grouping

Group	Treatment
Group I (Vehicle group)	Received 1% Saline
Group II (Negative control group)	Received MPTP (20 mg MPTP/kg b.w) i.p. as four injections in a single day at 2 h interval
Group III (Standard group)	Received MPTP (20 mg MPTP/kg body weight) i.p.+ Levodopa (100mg/kg)
Group IV (Treatment group)	Received MPTP (20 mg MPTP/kg body weight) i.p.+ SH4 (100mg/kg)
Group V (Treatment group)	Received MPTP (20 mg MPTP/kg body weight) i.p.+ SH9 (100mg/kg)

Behaviour Assessment:

Catalepsy Bar Test

According to Sandhir R. *et al.*, catalepsy bar test was used to measure muscular rigidity [13]. Animals were tested on a horizontal steel bar (15 cm long, diameter of 0.9 cm), which was kept at a height of 5.5 cm above the ground. The mouse was held by the tail during the test, and its front paws were placed on a steel bar and its back legs were placed on a flat surface. The descent latency was measured as time taken by the animals to correct the externally imposed posture. A cut-off time was 180 s, i.e., the trial was terminated if the animal did not exhibit any active paw movement.

Open Field Test

Animals spontaneous locomotor activity was evaluated using the open-field test. For open field test, a closed chamber (50 cm sides and height of 40 cm) was employed. Animals were placed in middle of the arena and observed for 3 min. Apparatus was cleaned with 95% (v/v) ethanol before use and cleaned again in between each test to remove odour cues. The data was recorded in terms of total distance travelled (m) and average velocity using ANY-maze™ video tracking software (Stoelting, Wood Dale, IL, USA).

Forced Swim Test

As previously mentioned, the forced swim test was utilized to assess depressive-like behaviour. Rats were kept in a water-filled cylinder (24°C), for 5 min. The test was recorded via a video camera and latency to stop and immobility duration were calculated. Depressive-like state was defined as an increase in the duration of immobility and decrease in latency to immobility.

Tail Suspension Test

Tail suspension test (TST) is an important behaviour test to determine a person's reaction to a stressful circumstance. To measure the length of immobility, the mouse tails were attached to a horizontal bar and kept there for six minutes. The length of time the person spends stationary will increase as depressive-like behaviour worsens. It should be mentioned that the TST is generally exclusively utilised on mice because of their smaller size and weight. To evaluate the antidepressant response, TSTs are used.

Sucrose Preference Test

The previously mentioned sucrose preference test was used to evaluate anhedonia. The test involved denying food and water to the animals for 18 hours before exposing them to two pre-weighted (separate) bottles for 1 hour each, one containing 3% sucrose solution and the other tap water. Sucrose preference was calculated according to the formula:

$$\text{Sucrose preference} = (\text{sucrose intake}/(\text{sucrose intake} + \text{water intake})) \times 100.$$

Reduced sucrose preference is suggestive of anhedonia and thus of depression-like behaviour. In addition, we also analysed the total sucrose and water consumption to compare general fluid intake between the groups.

Neurochemical Studies

Dissection and Homogenization

Following behavioural measurement, animals receiving chronic MPTP were cervically dislocated to death. The cerebellum and forebrain were eliminated along with the brains. Cortex, striatum, and subcortical portions of the brains were separated and weighed while the brains were placed on ice. In 0.1 M phosphate buffer (pH 8), a 10% (w/v) tissue homogenate was created.

Estimation of Lipid Peroxidation Products

By measuring TBARS, lipid peroxidation was spectrophotometrically calculated in brain tissue. In short, the Thio barbituric acid-Tri chloro acetic acid (TBA-TCA) reagent was added to the tissue homogenate supernatant for the measurement of TBARS before being fully mixed. For 15 minutes, the mixture was heated in a water bath. The tubes were centrifuged for 10 minutes after cooling, and the supernatant was removed for analysis. Using a UV spectrophotometer and a reagent blank, the produced color was read at 532 nm. Using 1,1,3,3-Tetra Methoxy Propane (TMP) and the standard curve, the amount of TBARS in the supernatant was calculated and expressed in nM/mg of protein.

Estimation of Reduced Glutathione (GSH)

1 ml of 10% TCA was used to precipitate 1 ml of tissue homogenate. Centrifugation was used to get rid of the precipitate. 4 ml of phosphate solution and 0.5 ml of the DTNB reagent were added to an aliquot of the supernatant. At 412 nm, the color produced was read. Standard reduced glutathione was used to create a standard curve to determine the quantity of GSH in the supernatant, which was then expressed in nM/mg of protein.

Determination of Dopamine Level:

Using UV-visible spectroscopy, the amount of dopamine in the entire brain was calculated. First, standard dopamine was serially diluted (from 50 to 500 ng/mL) to remove the standard linear dopamine curve. The dopamine detection range was set at 240–280 nm, and the conc. v/s. abs. linear curve was obtained. Each test group's supernatant was diluted ten times, and the presence of dopamine was determined by measuring the absorbance at 278 nm. The amount of dopamine present in the entire brain was calculated and represented in ng/g of tissue using the equation $y=mx+c$ derived from the linear curve and the sample absorbance [14].

Determination of Monoamine Oxidase Activity

Monoamine Oxidase-B Activity

Mitochondrial fractions for MAO-B assay were prepared from the striatum as described by Puka-Sundvall *et al.* [15]. Using a Potter-Elvehjam-type glass homogenizer, 10% (w/v) homogenate was made in ice-cold buffer A, which contains 10 mM Tris-HCl (pH 7.4), 0.44 M sucrose, 10 mM EDTA, and 0.1% (w/v) bovine serum albumin. The homogenate was then centrifuged at 2100 g for 15 min at 4°C. Further centrifugation of the supernatant was performed at 14,000 g for 15 min. at 4°C. The rough mitochondrial pellet was isolated, cleaned

with buffer A, and then centrifuged one more at 7000 g for 15 min at 4°C. The final mitochondrial pellet was re-suspended in buffer B, which contains 0.44 M sucrose and 10 mM Tris-HCl (pH 7.4). The technique described by Gupta *et al.* [16] was slightly modified to measure MAO-B activity. The particular MAO-B substrate, 4 mM benzylamine, was present in the assay mixture along with 2.75 ml of 0.1 M sodium phosphate buffer (pH 7.4). The reaction was started by adding mitochondrial fraction as a source of MAO-B, and the absorbance was measured for five minutes against a blank at a wavelength of 249.5 nm. The enzyme's activity was measured in nmol/min/mg protein.

Statistical Analysis

All values are expressed as mean \pm standard error mean (SEM). The Data was analyzed using a one-way analysis of variance (ANOVA) followed by Tukey's multiple comparison test. Values with $p < 0.05$ were considered as statistically significant.

Results and Discussion

Synthesis of Novel Compounds

In the present study, Ethyl 2-((5-(furan-2-ylmethylene)-4-oxothiazolidin-2-ylidene) amino)-thiazole-4-carboxylate (SH-4) was synthesised as presented in Scheme 1. N'-(4-(benzyloxy)-3-methoxybenzylidene)-2-acetamidothiazole-4-carbohydrazide (SH-9) was also prepared when equimolar quantity of 2-acetamido thiazole-4-carbohydrazide (13) was refluxed with substituted benzaldehyde 18 in the presence of absolute ethanol and few drops of glacial acetic acid for 14 hrs (Scheme 2). All compounds had IR, ¹H NMR/¹³C NMR and mass spectra in accord with their anticipated structures. The physical characterisation data of the compounds are given in Table 2.

Table 2: Physical Characterization Data of Synthesized Compounds

Compound Code	Mol. Formula	Appearance	Rf	Yield	Melting point
15	C ₈ H ₉ ClN ₂ O ₃ S	Light brown solid	0.8 (Chloroform: methanol: 9: 1)	87%	130-132°C
16	C ₉ H ₉ N ₃ O ₃ S ₂	Buff white solid	0.63 (Chloroform: methanol: 9: 1)	82%	190-192°C

SH4	C ₁₄ H ₁₁ N ₃ O ₄ S ₂	light yellow solid	0.58 (ethyl acetate: toluene 8:2)	73	190-192 °C
12	C ₈ H ₁₀ N ₂ O ₃ S	Buff white solid	0.65 (Toluene: Ethyl acetate: Formic acid: 5:4:1)	83 %	205-207 °C
13	C ₆ H ₈ N ₄ O ₂ S	White solid	0.76 (Chloroform: Ethanol: 7: 3)	54%	245-248 °C
SH9	C ₂₁ H ₂₀ N ₄ O ₄ S	milky white solid	0.64 (Chloroform: methanol: 9: 1)	79	182-184 °C

***In-silico* Study**

A molecular docking study and MMGBSA binding free energy calculation were carried out to better understand the molecular interactions of produced compounds (SH4 & SH9) with α -synuclein. The docking score and binding free energies of all the ligands were given in Table 3 and the 2D ligand interaction diagram of compounds SH4 & SH9, dopamine and Carbidopa were given in Figure 1.

Table 3: Molecular docking score and MMGBSA free-energy of binding of Dopamine, Carbidopa, SH4 and SH9 docked against α -synuclein

Compound	Glide Docking Score (kcal/mol)	MMGBSA ΔG binding (kcal/mol)
Dopamine (A)	-4.84	-19.83
Carbidopa (B)	-5.03	-23.71
SH-4 (C)	-6.78	-29.46
SH-9 (D)	-6.64	-25.94

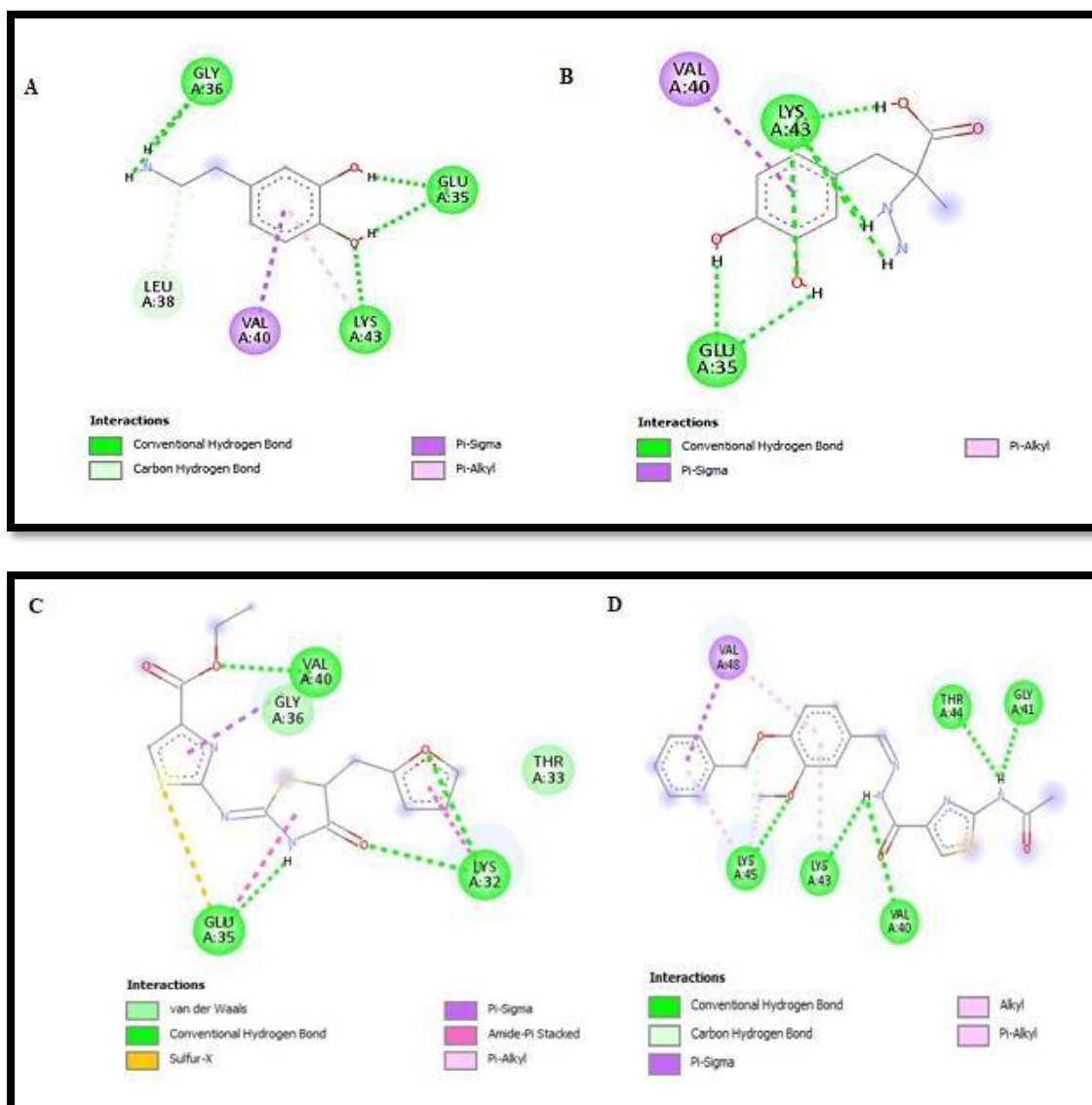


Figure 1: Two-dimensional receptor-ligand interaction diagram for Dopamine (A), Carbidopa (B), SH4 (C) and SH9 (D)

Compound SH-4 had the docking score of -6.78 kcal/mol and ΔG binding of -29.46 kcal/mol with α -synuclein indicated good inhibitory action against α -synuclein enzyme. The 2D ligand interaction diagram showed that this compound tightly binds to α -synuclein by forming π - π stacking. The compound SH9 had the docking score of -6.64 kcal/mol and ΔG binding of -25.94 kcal/mol which was nearly comparable but less than SH-4.

Behaviour Assessment:

In MPTP animals, muscular rigidity was significantly increased as compared to the control group. However, SH-4 & SH-9 groups treatment significantly reduced the muscular rigidity by 75% and 72%, respectively. The results were presented in figure 2. Open field test was used to

measure locomotor activity in terms of total distance travelled and average velocity. MPTP treated animals showed significant reduction in total distance travelled as compared to controls (Figure 3a and 3b). Additionally, average velocity was decreased in MPTP-treated mice while SH-4 and SH-9-treated animals showed no discernible change. Levodopa and MPTP effects were evaluated in connection to the forced swimming test (FST) immobility time. In order to assess the efficacy of various neurobiological drugs, the FST is a frequently used test in basic pharmacological research. The final 4 minutes of the FST, or a total of 6 minutes, saw no movement of the animals.

IFN was injected for six days, and for the same six days, MPTP was also given. The control groups were given saline as usual. Reduced animal immobility during the FST caused by the Levodopa was a definite indication of the antiparkinsonian effect (* $p < 0.05$). The compound Sh-4 also showed effect in compliance with levodopa. The results of FST were shown in figure 4. The amount of time spent immobile was slightly reduced by SH-4 & SH-9 compound (Figure 5). Levodopa, a common antiparkinson's drug, also demonstrated a notable (** $p < 0.001$) reduction in the time spent immobile. Moreover, the test compounds i.e., SH-4, showed significant decrease (* $p < 0.05$) in a time of immobility closed to Levodopa. The results of the sucrose preference test likewise supported those of the MPTP induced anhedonia in mice, selected compounds improved the preference. The results obtained with SH-4 virtually supported the antiparkinsonian results. Results of Sucrose preference test were presented in figure 6.

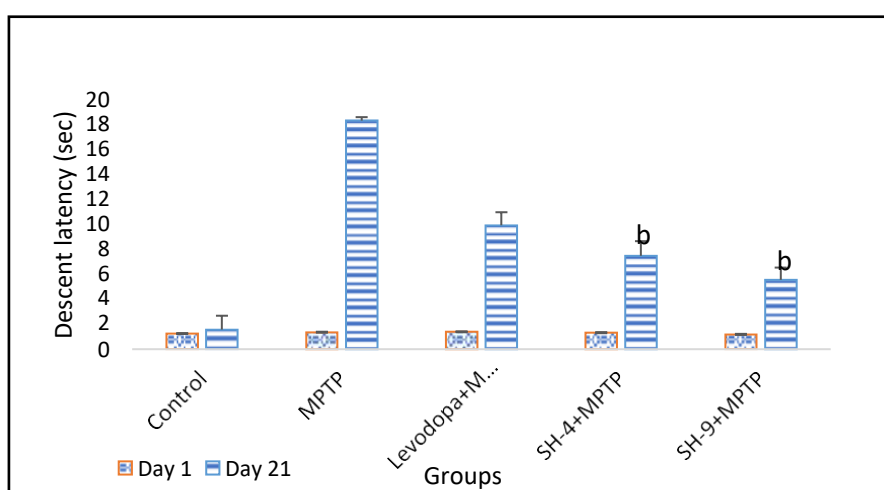


Figure 2: Effect of SH-4 and SH-9 treatment on muscular rigidity assessed by catalepsy bar test in MPTP-induced model of PD. Values are expressed as mean \pm SEM; $n = 6/$

group; 'a' represents significant difference from control group ($p < 0.05$); 'b' represents significant difference from MPTP group ($p < 0.05$).

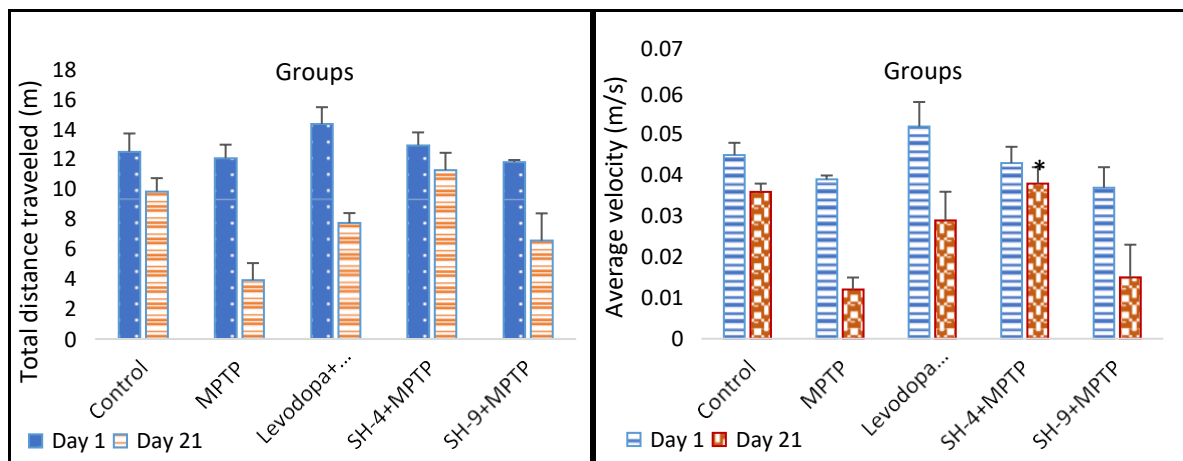


Figure 3: Effect of SH-4 & SH-9 treatment on motor functions assessed using open field test in MPTP mice model of PD. Total distance travelled (A) and Average velocity (B). Values are expressed as mean \pm SEM; $n = 6/$ group; A significant difference was seen in SH-4 group when compared with MPTP group ($p < 0.05$).

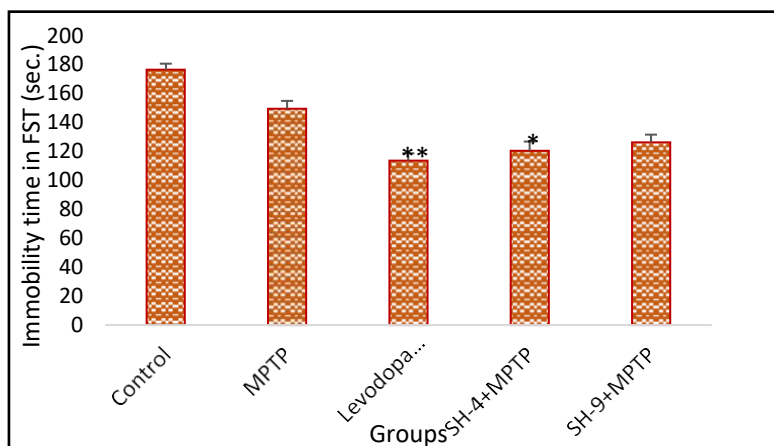


Figure 4: Effect of SH-4 & SH-9 treatment on motor functions assessed using Forced swim test in MPTP mice model of PD. Values are expressed as mean \pm SEM; $n = 6/$ group; A significant activity was shown by Levodopa (** $p < 0.001$) and SH-4 group (* $p < 0.05$) in comparison to MPTP group.

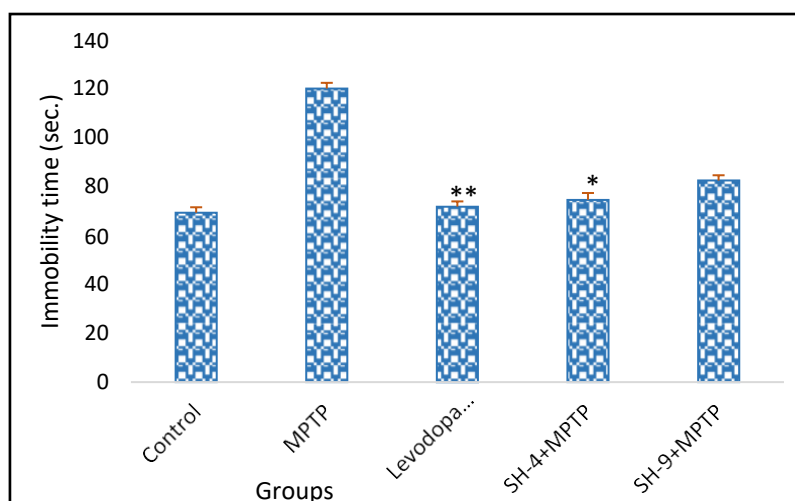


Figure 5: Effect of SH-4 & SH-9 treatment on motor functions assessed using Tail suspension test in MPTP mice model of PD. Values are expressed as mean \pm SEM; n = 6/group; A significant activity was shown by Levodopa (**p<0.001) and SH-4 group (*p < 0.05) in comparison to MPTP group.

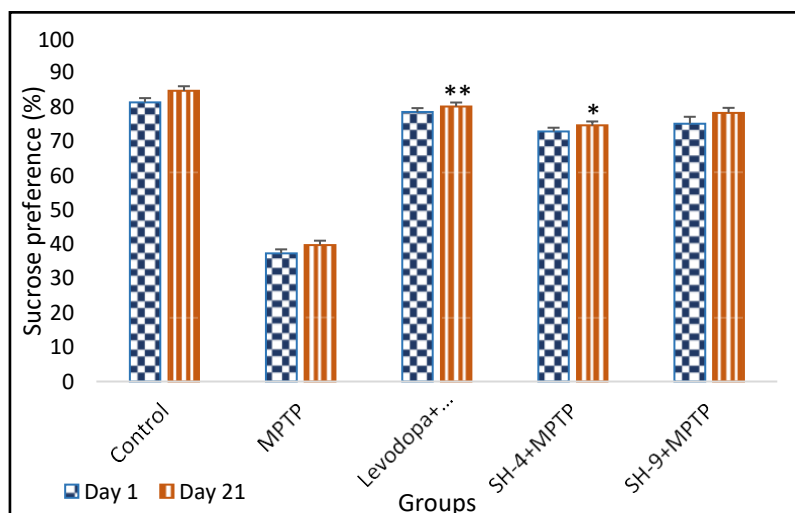


Figure 6: Effect of SH-4 & SH-9 treatment on motor functions assessed using Sucrose preference test in MPTP mice model of PD. Values are expressed as mean \pm SEM; n = 6/group; A significant activity was shown by Levodopa (**p<0.001) and SH-4 group (*p < 0.05) in comparison to MPTP group.

Biochemical Evaluation

Alzheimer's, Parkinson's, and Huntington's disease are just a few of the neurodegenerative conditions that have been linked to cellular redox imbalance. Due to its high oxygen

consumption, abundance of polyunsaturated fatty acids, transition metals, and relatively low amounts of antioxidant enzymes, the brain is particularly vulnerable to oxidative stress [17]. Changes in the levels of antioxidant enzymes and LPO in PD patients as well as in animal models provide evidence for the significance of the antioxidant system in the disease. Chronic use of neuroleptics increases the production of free radicals, which causes oxidative stress and has been linked to the pathogenesis of Parkinson's disease (PD).

According to our findings, MPTP, a neurotoxic, increased LPO while lowering GSH levels and antioxidant enzyme (SOD and GSH-Px) activity in brain homogenate. A decrease in GSH may hinder the removal of H₂O₂ and encourage the creation of OH•, which raises the free radical load, causes oxidative stress, and subsequently disturbs homeostasis. When given 30 minutes prior to MPTP, the compounds SH-4 and SH-9 greatly reduced oxidative stress, restoring enzyme activity as well as GSH and MDA levels to levels that were nearly identical to the control (Figures 7a and 7b). Dopamine levels were dramatically raised by both substances, SH-4 and SH-9 (Figure 7c). Animals from each group had the striatum's MAO-B activity measured. When compared to control mice, MPTP-treated animals' MAO-B activity was dramatically elevated by about 66%. The MAO-B activity, however, was significantly reduced in the animal treated with SH-4 and SH-9 (Figure 7d).

Discussion

Levodopa and certain MAO-B inhibitors are now used as PD therapy. Using an *in silico* molecular docking technique, the inhibitory potential of two produced compounds, SH-4 and SH-9, was investigated. Both substances bind to α -synuclein, according to the findings of the molecular docking experiment. By occupying the enzyme's active site and generating hydrogen bonds, SH-4 and SH-9 create the most stable complex with α -synuclein. The synthetic substances were taken orally 30 minutes before MPTP was given. Significant motor abnormalities were caused by acute MPTP treatment to mice, which is consistent with other research showing motor impairments following acute MPTP poisoning [18–19]. As determined by the catalepsy bar test, forced swim test, sucrose preference test, and open field test, pre-treatment with SH-4 and SH-9 alleviated motor deficits. Behavioral immobility known as catalepsy is characterized by tight muscles and a person's inability to maintain their position for an extended period of time. Given that PD and schizophrenia patients exhibit a comparable behavioral disorder, catalepsy has significant clinical implications [20].

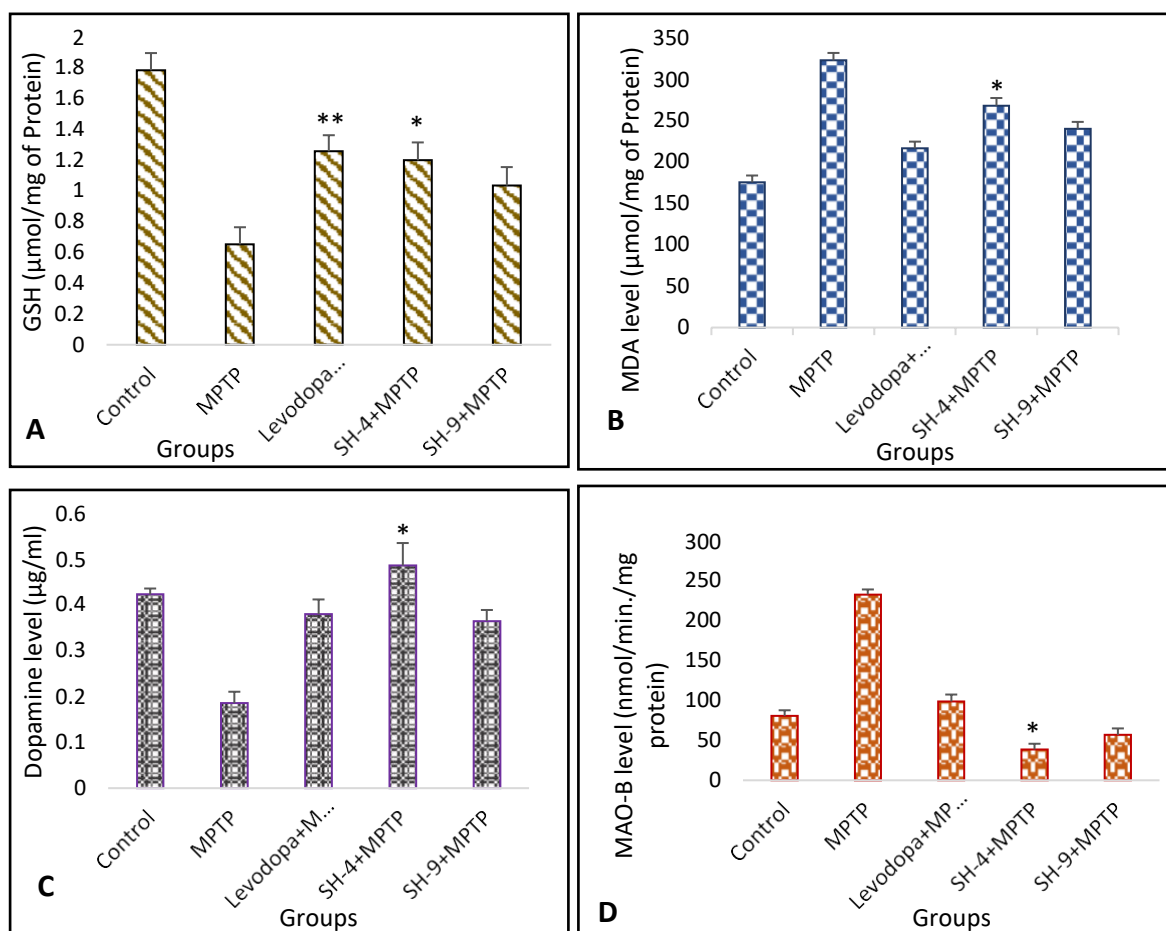


Figure 7: Effect of Compounds SH-4 & SH-9 on biochemical parameters. A. GSH, B. LPO, C Dopamine level and D. MAO-B level. * $p < 0.05$, ** $p < 0.01$ when compared to MPTP mice model of PD.

In the current investigation, mice treated with MPTP showed a considerable increase in descent latency, which was reduced by the addition of SH-4 and SH-9. Mice exposed to MPTP crossed the beam considerably slower than the control group. However, supplementation with SH-4 and SH-9 reduced the time it took the animals to cross the beam and concurrently increased the average speed. According to an *in-vivo* investigation, the MPTP-induced PD model's brain has elevated MAO-B activity, which is consistent with the increased MAO-B activity that has been observed in the brains of PD patients. However, the activity of MAO-B was decreased in mice treated with MPTP and given SH-4 and SH-9.

Conclusion

In conclusion, the present study demonstrated potential of SH-4 & SH-9 compounds as an anti-parkinsonian molecule that enhances Dopamine levels in brain through inhibition of MAO-B activity. Moreover, both compounds also alleviated motor impairments in MPTP intoxicated mice. Additionally, the anti-oxidant and anti-inflammatory capabilities of synthetic substances

like SH-4 and SH-9 may possibly be responsible for their neuroprotective effects. As far as we are aware, this is the first work to suggest SH-4 & SH-9 as an inhibitor of α -synuclein utilizing both an animal model of PD and an *in silico* model. In our study, the chemical SH-4 demonstrated more encouraging findings than SH-9. The study's conclusions are crucial for the development of these chemicals as prospective treatments for PD and other diseases where MAO-B may be a target.

References:

1. Forno LS. The Neuropathology of Parkinson's Disease: The Lewy body as a clue to the nerve cell degeneration. *Progress in Parkinson research*. 1988;11-21.
2. Armstrong MJ, Okun MS. Diagnosis and treatment of Parkinson disease: a review. *Jama*. 2020;323(6):548-60.
3. Chopade P, Chopade N, Zhao Z, Mitragotri S, Liao R, Chandran Suja V. Alzheimer's and Parkinson's disease therapies in the clinic. *Bioengineering & Translational Medicine*. 2023;8(1): 1-23.
4. Martin LJ, Pan Y, Price AC, Sterling W, Copeland NG, Jenkins NA, Price DL, Lee MK. Parkinson's disease α -synuclein transgenic mice develop neuronal mitochondrial degeneration and cell death. *Journal of Neuroscience*. 2006;26(1):41-50.
5. Braak H, Del Tredici K, Rüb U, De Vos RA, Steur EN, Braak E. Staging of brain pathology related to sporadic Parkinson's disease. *Neurobiology of aging*. 2003;24(2):197-211.
6. R.M. Geha, I. Rebrin, K. Chen, J.C. Shih. Substrate and inhibitor specificities for human monoamine oxidase A and B are influenced by a single amino acid. *J. Biol. Chem*. 2000; 276:9877-9882.
7. P. Riederer, G. Laux. MAO-inhibitors in Parkinson's disease. *Exp. Neurobiol*. 2011; 20:1-17.
8. J.P.M. Finberg, J.M. Rabey. Inhibitors of MAO-A and MAO-B in psychiatry and neurology. *Front. Pharmacol.*, 7 (2016), p. 340.
9. J.J. Chen, J.R. Wilkinson. The monoamine oxidase type B inhibitor rasagiline in the treatment of Parkinson disease: is tyramine a challenge? *J. Clin. Pharmacol.*, 52 (2012), pp. 620-628.
10. Ejaz S, Nadeem H, Paracha RZ, Sarwar S, Ejaz S. Designing, synthesis and characterization of 2-aminothiazole-4-carboxylate Schiff bases; antimicrobial evaluation against multidrug resistant strains and molecular docking. *BMC Chem*. 2019 Sep 14;13(1):115. doi: 10.1186/s13065-019-0631-6. PMID: 31535091; PMCID: PMC6744641.
11. Morris GM, Huey R, Lindstrom W, Michel FS, Richard KB et al. (2009) AutoDock4 and AutoDockTools4: Automated docking with selective receptor flexibility. *Journal of Computational Chemistry* 30: 2785–2791. Link:<https://bit.ly/3Dew62s>.
12. D. Huang, J. Xu, J. Wang, J. Tong, X. Bai, H. Li, Z. Wang, Y. Huang, Y. Wu, M. Yu, F. Huang, Dynamic changes in the nigrostriatal pathway in the MPTP mouse model of Parkinson's disease, *Parkinson's Dis*. 2017 (2017) 1–7.
13. Pathania, A., Kumar, R., & Sandhir, R. (2021). Hydroxytyrosol as anti-parkinsonian molecule: Assessment using in-silico and MPTP-induced Parkinson's disease model. *Biomedicine & Pharmacotherapy*, 139, 111525.

14. Ojha, P.S., Biradar, P.R., Tubachi, S. *et al.* Evaluation of neuroprotective effects of *Canna indica* L against aluminium chloride induced memory impairment in rats. *ADV TRADIT MED (ADTM)* **23**, 539–556 (2023). <https://doi.org/10.1007/s13596-021-00627-x>.
15. Malgorzata Puka-Sundvall, Camilla Wallin, Eric Gilland, Ulrika Hallin, Xiaoyang Wang, Mats Sandberg, Jan-Olof Karlsson, Klas Blomgren, Henrik Hagberg, Impairment of mitochondrial respiration after cerebral hypoxia–ischemia in immature rats: relationship to activation of caspase-3 and neuronal injury, *Developmental Brain Research*, 125 (1–2), 2000, 43-50.
16. D. Gupta, Y. Kurhe, M. Radhakrishnan. Antidepressant effects of insulin in streptozotocin induced diabetic mice: modulation of brain serotonin system. *Physiol. Behav.*, 129 (2014), pp. 73-78.
17. Faizul Azam, Bashir A. El-gnidi, Ismail A. Alkskas & Musa A. Ahmed (2010) Design, synthesis and anti-Parkinsonian evaluation of 3-alkyl/aryl-8-(furan-2-yl)thiazolo[5,4-e] [1,2,4]triazolo[1,5-c]pyrimidine-2(3H)-thiones against neuroleptic-induced catalepsy and oxidative stress in mice, *Journal of Enzyme Inhibition and Medicinal Chemistry*, 25:6, 818-826, DOI: 10.3109/14756361003671052.
18. R.P. Ojha, M. Rastogi, B.P. Devi, A. Agrawal, G.P. Dubey. Neuroprotective effect of curcuminoids against inflammation-mediated dopaminergic neurodegeneration in the mptp model of Parkinson's disease. *J. Neuroimmune Pharmacol.*, 7 (2012), pp. 609-618.
19. G.E. Meredith, D.J. Rademacher. MPTP mouse models of Parkinson's disease: an update. *J. Parkinson's Dis.*, 1 (2011), pp. 19-33
20. E.S. Tauber, L.G. Lewis, O.R. Langworthy. Vesical activity in schizophrenic states associated with catalepsy. *Arch. Neurol. Psychiatry*, 39 (1938), pp. 14-23.